

# miR-539-5p Regulates Irritable Bowel Syndrome Pathological Processes by Targeting KDM6A

Yiqun Li<sup>1</sup> , Zhiyu Wang<sup>1</sup> , Shuangshuang Zhang<sup>1</sup> , Yanling Hua<sup>1</sup> , Xinting Fan<sup>1</sup> , Li Li<sup>2</sup> 

<sup>1</sup>Institute of Digestive Diseases, Xuzhou Medical University, Jiangsu, China

<sup>2</sup>Department of Gastroenterology, The Affiliated Hospital of Xuzhou Medical University, Jiangsu, China

**Cite this article as:** Li Y, Wang Z, Zhang S, Hua Y, Fan X, Li L. MiR-539-5p regulates irritable bowel syndrome pathological processes by targeting KDM6A. *Turk J Gastroenterol*. Published online September 10, 2025. doi: 10.5152/tjg.2025.24684.

## ABSTRACT

**Background/Aims:** The chronicity and recurrence of irritable bowel syndrome (IBS) pose significant burdens on patients' lives, making it urgent to understand its underlying mechanisms. This study intends to investigate the function and regulatory mechanisms of miR-539-5p in IBS and lay the foundation for the creation of more effective therapeutic strategies.

**Materials and Methods:** Rat model of IBS with diarrhea (IBS-D) was established and evaluated by the abdominal withdrawal reflex. The IBS cellular model was established in vitro using lipopolysaccharide (LPS), and real-time quantitative polymerase chain reaction was used to assess the changes in the miR-539-5p expression. Cell counting kit-8 assays, flow cytometry, and enzyme-linked immunosorbent assay were used to evaluate the effects of different treatments on cell viability, paracellular permeability, apoptosis, and inflammatory responses. Bioinformatics techniques and dual-luciferase reporter gene assays were leveraged to forecast and confirm the interaction between miR-539-5p and the KDM6A gene.

**Results:** In IBS-D rats, miR-539-5p was conspicuously downregulated, and miR-539-5p overexpression could improve the symptoms of rats. Under exposure to LPS, the expression of miR-539-5p was evidently decreased. Upregulating miR-539-5p could significantly mitigate LPS-induced cellular damage, namely inhibiting the apoptosis of intestinal mucosal epithelial cells, promoting cell proliferation, reducing paracellular permeability, and suppressing the inflammatory response. KDM6A, as the target gene of miR-539-5p, was remarkably upregulated in IBS-D rats and cells exposed to LPS. KDM6A overexpression counteracts the protective effects mediated by the upregulation of miR-539-5p.

**Conclusion:** miR-539-5p may be involved in regulating the pathological processes of IBS-D by targeting KDM6A.

**Keywords:** Cell behavior, IBS, inflammatory response, KDM6A, LPS, miR-539-5p

## INTRODUCTION

Irritable bowel syndrome (IBS) is a prevalent functional gastrointestinal disorder characterized by abdominal pain, bloating, or discomfort, often accompanied by alterations in bowel habits or stool consistency.<sup>1,2</sup> Based on stool features, IBS can be further categorized into 3 subtypes: IBS-D (diarrhea-predominant), IBS-C (constipation-predominant), and IBS-M (mixed). These subtypes respectively denote patients whose primary symptoms are diarrhea, constipation, or an alternating pattern between the 2.<sup>3</sup> The pathophysiology of IBS is multifaceted. It encompasses imbalances in the intestinal flora, impairments in the intestinal mucosal barrier function, low-grade intestinal inflammation, and aberrations in brain-gut axis communication. Given the varied and recurrent nature of IBS manifestations, it considerably diminishes patients' quality of life.<sup>4</sup> Currently, the precise pathogenesis of IBS remains unknown, making in-depth investigation of its molecular mechanisms crucial for

overcoming research hurdles, improving understanding, and addressing the disease.

In the field of molecular biology, microRNAs (miRNAs) have been recognized as crucial regulators of various biological processes, which are also involved in disease conditions. The expression profiles of miRNAs in serum, intestinal mucosa, and other tissues of IBS patients undergo alterations, potentially reflecting the pathophysiological status of IBS.<sup>5,6</sup> For instance, the expression of miR-19b in intestinal epithelial cells and its regulatory role over suppressor of cytokine signaling 3 are crucial for intestinal mucosal injury repair.<sup>7</sup> A study has indicated that miR-155-5p is implicated in the pathophysiological mechanisms of IBS, and inhibiting its expression can elevate the visceral pain threshold in IBS mouse models.<sup>8</sup> Zhou et al have suggested that miR-199 holds potential as a therapeutic agent for addressing visceral hyperalgesia in patients with IBS.<sup>9</sup> Further investigation into the

Corresponding author: Li Li, Yiqun Li, e-mail: lily9711214@126.com, liyiqun22@163.com

Received: November 11, 2024 Revision requested: December 19, 2024 Last revision received: January 17, 2025 Accepted: January 22, 2025

Publication Date: September 10, 2025

DOI: 10.5152/tjg.2025.24684



Copyright © Author(s) – Available online at <https://www.turkjgastroenterol.org>.

Content of this journal is licensed under a Creative Commons Attribution (CC BY) 4.0 International License

functions and regulatory mechanisms of miRNAs holds significant promise in elucidating the pathogenesis of IBS.

As an emerging miRNA molecule, miR-539-5p has attracted considerable focus due to its broad regulatory functions in key biological processes.<sup>10-12</sup> Among these, its function in intestinal-related diseases is of particular interest. In colorectal cancer, miR-539-5p has been identified to exhibit a notable association with the malignant characteristics of cancer cells.<sup>13</sup> Additionally, during the pathological process of pediatric pneumonia complicated by diarrhea, miR-539-5p expression undergoes marked downregulation, correlating with inflammatory responses in intestinal epithelial cells.<sup>14</sup> Furthermore, in the context of inflammatory bowel diseases, miR-539-5p effectively mitigate cellular pyroptosis and inflammatory reactions by modulating the NLRP3/caspase-1 signaling pathway.<sup>15</sup> However, the specific mechanistic underpinnings of miR-539-5p in IBS remain elusive.

Given the complexity of IBS and the potential role of miR-539-5p in intestinal diseases, this study investigates the regulatory mechanisms of miR-539-5p in colonic mucosal epithelial cells within the context of IBS by utilizing rat and cellular models. The objective is to gain further insights into the pathogenesis of IBS and to facilitate the development of new therapeutic targets.

## MATERIALS AND METHODS

### Animals

Five specific pathogen free-grade SD pregnant rats, each weighing ( $360 \pm 20$ ) grams and at a gestational age of ( $18 \pm 1$ ) days, were purchased from the Experimental Animal Center of the Chinese Academy of Sciences (Shanghai, China). The rats were kept under optimal conditions, with indoor temperatures maintained at ( $22 \pm 2$ )°C and humidity approximately 50%, ensuring ad libitum access to food and water. Following parturition, 50 pups were born, and

healthy ones were selected for subsequent experimental procedures.

The study was authorized by the Xuzhou Medical University Animal Ethics Committee (No. 202503T030, Date: February 15, 2025), adhering strictly to globally accepted ethical principles and the institution's regulations concerning animal care and experimentation. This article does not contain any studies with human subjects performed by any of the authors, informed consent statement is not required.

### Establishment of the Rat Model of Irritable Bowel Syndrome and Grouping

The objective of this study is to develop a rat model of IBS-D that more closely resembles clinical scenarios by simulating multiple etiological factors. Refer to the specific methodologies outlined in the study by Wang et al.<sup>16</sup> From postnatal day 2 to day 15, pups were separated from their mothers for 3 hours daily at a fixed time, simulating the effects of early-life stress on gut development and function. At 35 days of age, pups underwent fasting with free access to water for 12 hours. Subsequently, a 1 mm diameter, single-lumen central venous catheter lubricated with paraffin oil was inserted 4 cm into the colon via the anus. A slow infusion of 1 mL of 4% acetic acid solution was administered to elicit colonic inflammation, followed immediately by tail elevation for 60 seconds to facilitate even distribution. The colon was then flushed with 1 mL of phosphate buffered saline (PBS) to mitigate residual irritation. Commencing 3 days after the acetic acid challenge (i.e., at 38 days of age), pups were subjected to chronic restraint stress. Using non-restrictive tape, their upper bodies were gently restrained to limit their ability to groom their faces with their forelimbs. This restraint lasted 2 hours daily for 7 consecutive days, simulating the effects of chronic psychological stress on gut function.

Thirty-two healthy pups were randomly and equally divided into 4 groups. The first group, designated as the control, was reared under standard conditions to ensure their health. The second group underwent the establishment of an IBS-D model, with the specific methodology detailed previously. The third group received concurrent injections of acetic acid and 0.4 mL of PBS into the peritoneal cavity, serving as the negative control (NC) for miR-539-5p upregulation, maintaining all other rearing protocols identical to those of the second group. The fourth group, alongside the acetic acid injection,

### Main Points

- *miR-539-5p is downregulated in irritable bowel syndrome with diarrhea (IBS-D) rats, and its overexpression alleviates IBS-D symptoms.*
- *Overexpression of miR-539-5p protects against LPS-induced intestinal mucosal epithelial cell damage.*
- *Kdm6a, a target of miR-539-5p, is significantly upregulated in IBS-D rats.*
- *Overexpression of KDM6A reverses the protective effects of miR-539-5p on cells.*

administered an intra-peritoneal injection of miR-539-5p mimic (dissolved at 5 mg/kg in 0.4 mL of PBS) to augment miR-539-5p expression, with all other rearing conditions mirroring those of the second group.

### **Model Evaluation and Validation**

On the first day following the establishment of the model (at 45 days of age), the efficacy of modeling was validated. The rats were given free access to water and fasted for 12 hours, during which the minimum volume threshold required to elicit an abdominal withdrawal reflex (AWR) score of 3 upon colorectal balloon distension under sevoflurane anesthesia was measured and designated as the AWR minimum volume threshold. A marked decrease in this threshold indicated successful modeling. The AWR scoring system, designed to assess visceral sensitivity in rats, was evaluated by 2 independent observers using a double-blind approach. The scoring criteria were as follows: 0 points for no observable response during balloon distension, 2 points for brief head movement with subsequent cessation, 3 points for abdominal muscle contraction, and 4 points for pronounced abdominal contraction accompanied by arching of the back and pelvic elevation.<sup>16</sup> Following the confirmation of successful modeling, abdominal aortic blood was collected from the rats, which were then euthanized in accordance with established protocols.

### **Determination of Serum Inflammatory Factors in Rats by Enzyme-Linked Immunosorbent Assay**

Blood samples were processed by centrifugation at 4°C (20 minutes) and the resulting serum (supernatant) was stored at -80°C for analysis. To quantify the levels of interleukin-1 $\beta$  (IL-1 $\beta$ ), IL-6, and tumor necrosis factor- $\alpha$  (TNF- $\alpha$ ) in the serum, an enzyme-linked immunosorbent assay (ELISA) assay (Jianglai Biotechnology Co., LTD, Shanghai, China) is performed following the manufacturer's instructions. Standard solutions are diluted into 5 gradients, with 50  $\mu$ L of each gradient dispensed into designated wells. The plate is incubated at 37°C for 30 minutes under a sealed plate membrane, followed by washing with PBS. After drying, equal volumes of chromogenic reagent A and reagent B are sequentially added to each well, gently mixed, and incubated at 37°C for 10 minutes in the dark for color development. After the reaction was terminated, a microplate reader (Thermo Fisher Scientific, Waltham, MA, USA) was used to detect the absorbance at 450 nm (OD<sub>450</sub>) and calculate the levels of inflammatory factors.

### **Determination of Serum D-Lactic Acid and Diamine Oxidase in Rats by Enzyme-Linked Immunosorbent Assay**

The levels of D-lactic acid (D-LA) and diamine oxidase (DAO) in rat serum were quantitatively determined using ELISA method. Adhering strictly to the detailed instructions provided in the kit (D-LA ELISA kit, and DAO ELISA kit, Jianglai Biotechnology Co., LTD, Shanghai, China), the pretreatment and dilution steps were carried out meticulously. Throughout the experimental procedure, rigorous control was exercised over the reaction conditions, encompassing temperature, duration, as well as the precise order and volume of reagent addition. Ultimately, the OD<sub>450</sub> values were measured, which served as the basis for the scientific assessment of D-LA and DAO concentrations in the rat serum samples. The specific methods refer to the study by Zhu et al.<sup>17</sup> the specific methods refer to the study by Zhu et al. and the ELISA kit instructions.

### **Cell Culture and Lipopolysaccharide (LPS) Induction**

The NCM460 cell line, derived from human colonic mucosal epithelium, was sourced from the Cell Resource Center at the Shanghai Institutes for Biological Sciences in China. It was stored at -80°C and thawed prior to use. The cells were cultivated in Dulbecco's modified eagle medium (DMEM) (Gibco, USA), enriched with 10% fetal bovine serum and 1% double antibiotics, maintained at 37°C, 5% CO<sub>2</sub>. Upon reaching approximately 80% confluence in culture dishes, subculturing was performed. The fourth generation NCM460 cells, which were in logarithmic growth, were taken and inoculated in 24-well plates. The cells were then incubated in the above incubator until they adhered to the plate surface. After attachment, the cells were exposed to varying concentrations of LPS (0, 2, 4, and 8  $\mu$ g/mL, Sigma-Aldrich, St. Louis, MO, USA) for a duration of 24 hours, simulating an IBS-like environment. Refer to the specific methodologies outlined in the study by Zhang et al.<sup>18</sup>

### **Cell Transfection**

NCM460 cells treated with 8  $\mu$ g/mL LPS and in good culture were screened and divided into the miR-539-5p overexpression group (miR-mimic), the miR-539-5p low expression group (miR-inhibitor) and its NC group (miR-NC), the KDM6A overexpression group (pcDNA3.1-KDM6A) and its NC group (pcDNA3.1), and a blank control group was also set up. Lipofectamine 2000 (Invitrogen, Carlsbad, USA) was utilized for transfection. Under the guidance of the instructions, the transfection reagent

and plasmid were used to prepare transfection complexes and transfected into each group of cells respectively. After culturing in the incubator for 48 hours, the transfected cells that were successfully obtained were screened through real-time quantitative polymerase chain reaction (RT-qPCR) analysis.

### **Real-Time Quantitative Polymerase Chain Reaction**

Total RNA was extracted from rat serum and various cell groups employing the Trizol method (Tiangen Biochemical Technology Co., Ltd., Beijing, China). Specifically, 1 mL of TRIzol reagent was added to each tissue sample (weighing between 50 and 100 mg) or to cells grown in 6-well plates. These samples were then transferred to 1.5 mL Eppendorf tubes for lysis. Following lysis, 200  $\mu$ L of chloroform was introduced and the mixture was centrifuged. Subsequently, the upper aqueous phase, containing the RNA, was transferred to a fresh 1.5 mL Eppendorf tube. An equal volume of isopropanol was added to this tube, and the solution was refrigerated at  $-20^{\circ}\text{C}$  for 1 hour to precipitate the RNA. After rinsing with anhydrous ethanol, the RNA was dissolved in 20  $\mu$ L of Rase-free double distilled water. The concentration and purity of the RNA were assessed using a Nanodrop2000 ultramicro spectrophotometer. Reverse transcription was conducted utilizing the PrimeScript<sup>®</sup> RT Master Mix Perfect Real Time Reagent Kit (Vazyme Biotech Co., Ltd., Nanjing, China). The reverse transcription system adhered to the recommended 20  $\mu$ L volume (supplementary table 1), The reaction program was carried out at  $37^{\circ}\text{C}$ , 15 minutes;  $85^{\circ}\text{C}$ , 5 seconds; and  $4^{\circ}\text{C}$ , forever. The resulting cDNA was diluted 50-fold for use in RT-qPCR reactions. The RT-qPCR was executed with the RT-qPCR kit (Vazyme Biotech Co., Ltd., Nanjing, China) on a thermocycler. The specific reaction system and reaction procedure are shown in supplementary tables 2 and 3, respectively. In addition, each reaction was performed with 5 replicates. Upon completion, the relative expression levels of miRNAs (normalized to *U6*) and mRNAs (normalized to glyceraldehyde-3-phosphate dehydrogenase) were calculated using the  $2^{-\Delta\Delta\text{Ct}}$  method. All amplification primers for this experiment were synthesized by Sangon Biotech Biological Co. (Shanghai, China), and their sequences are provided in supplementary table 4.

### **Cell Proliferation**

Trypsin was used to detach successfully transfected cells from the dish. The cells were subsequently transferred to a 96-well plate with a density of  $1 \times 10^3$  cells per well for further incubation in incubator. At the indicated time

points (0, 24, 48, and 72 hours), 10  $\mu$ L of cell counting kit-8 reagent (Dojindo Laboratories, Kumamoto, Japan) was introduced to each well and thoroughly mixed. Following a 4-hour period of additional incubation, allowing for the complete reaction, the optical density of each well was measured at a wavelength of 450 nm ( $\text{OD}_{450}$ ) using a spectrophotometer (MultiskanGo, Thermo Scientific, Waltham, MA, USA).

### **Determination of Paracellular Permeability**

To assess the paracellular permeability of NCM460 cells, a monolayer of intestinal epithelial barrier was established. Drawing on the research of Gregorio,<sup>19</sup> Kida et al,<sup>20</sup> the specific steps are as follows: NCM460 cells in control group and transfection group were carefully selected, digested, counted, and adjusted to a concentration of  $1 \times 10^5$  cells per milliliter. These cells were then seeded in the upper chamber of Transwell (Costar, Corning, NY, USA), with the basolateral compartment being supplemented with complete DMEM. The cells were incubated at  $37^{\circ}\text{C}$  with 5%  $\text{CO}_2$  until a stable monolayer barrier was achieved, confirmed by assessing transmembrane electrical resistance. Subsequently, LPS was introduced into both the apical and basolateral chambers, and the cells were further incubated for 24 hours. Then, 1 mg/mL of fluorescein isothiocyanate-dextran (FITC-dextran; Sigma-Aldrich, St. Louis, MO, USA) was introduced into the upper chamber and allowed to equilibrate for 2 hours under the same incubation conditions. Following this, 100  $\mu$ L of culture medium from the lower chamber was carefully aspirated, and its OD was measured utilizing a fluorescence spectrophotometer (Hitachi, Tokyo, Japan) at excitation wavelength of 485 nm and an emission wavelength of 535 nm. Relative paracellular permeability was calculated using the method of Susan et al.<sup>21</sup>

### **Cell Apoptosis**

The cells were isolated using trypsin, followed by a wash step. After resuspension in an appropriate amount of binding buffer, 5  $\mu$ L of Annexin V-FITC and Propidium Iodide (PI) were added to the cell suspension according to the requirements of the staining reagent instructions (Sobo Technology Co., Ltd., Beijing, China). Following the mixing process, the solution was incubated at normal room conditions for a period of 30 minutes, ensuring that the incubation took place in an environment devoid of light. Finally, the apoptosis rate of the cells was analyzed and assessed with a FACS Calibur flow cytometer (BD Biosciences, San Jose, USA).



### Luciferase Reporter Gene Assay

Firstly, primers were designed based on the predicted binding site to PCR-amplify 3'UTR fragments containing and lacking the miR-539-5p- and *KDM6A*-binding domain. The amplified products were then purified and tested. The purified 3'UTR fragments, both wild-type and mutant, were separately digested with enzymes and ligated into the pmirGLO dual-luciferase reporter vector. These constructs were transformed into competent cells to screen positive clones, which were further verified by colony PCR and sequencing to obtain wild-type (WT)-*KDM6A* and mutant (MUT)-*KDM6A* plasmids. According to transfection protocols, miR-mimic, miR-inhibitor, and miR-NC transfection complexes were prepared and co-transfected into NCM460 cells with either the WT-miR-539-5p or MUT-miR-539-5p plasmids. Following a 6-hour incubation period, the medium was exchanged for complete DMEM, and the cells were allowed to culture for a further 48 hours, during which cell condition was monitored and the culture environment was maintained. Following the incubation process, the cells were lysed and luciferase substrates were added to determine the relative luciferase activity.

### Bioinformatics Analysis

The downstream target genes of miR-539-5p were mined using TargetScan ([https://www.targetscan.org/vert\\_80/](https://www.targetscan.org/vert_80/)), miRDB (<https://mirdb.org/>), and miWalk (<http://mirwalk.umm.uni-heidelberg.de/>). The obtained target genes were used to draw a Venn diagram with graphing software. The functional annotations of gene ontology (GO) and Kyoto Encyclopedia of Genes and Genomes (KEGG) pathways were based on the DAVID bioinformatics tool of the National Institutes of Health (<https://david.ncicrf.gov/summary.jsp>), and a visualized mRNA-protein-protein interaction (PPI) network was constructed using STRING ([https://cn.string-db.org/cgi/input?sessionId=bHo5PiOTRAjM&input\\_page\\_show\\_search=off](https://cn.string-db.org/cgi/input?sessionId=bHo5PiOTRAjM&input_page_show_search=off)).

### Statistical Analysis

The data were processed and visualized using GraphPad Prism version 9.3.1, (GraphPad Software, Inc., San Diego, CA, USA) with the measurement outcomes presented as mean  $\pm$  standard deviation ( $\bar{x} \pm SD$ ). For comparisons across multiple groups, a 1-way ANOVA test was conducted, followed by Tukey's post hoc test. Statistical significance was determined at a *P*-value threshold of  $< .05$ .

## RESULTS

### Construction of Irritable Bowel Syndrome with Diarrhea Rat Model

Successfully established IBS-D rat models exhibited a notable decrease in AWR minimum volume threshold, accompanied by compromised intestinal barrier function and inflammatory responses. Compared to normal rats, IBS-D rats demonstrated a significant downregulation of miR-539-5p expression (Figure 1A). However, transfection with miR-539-5p mimics caused a marked enhancement of the AWR minimum volume threshold in IBS-D rats (Figure 1B), together with suppression of D-LA levels (Figure 1C), DAO activity (Figure 1D) and pro-inflammatory cytokine production (Figure 1E).

### Construction of an Intestinal Mucosal Epithelial Cell Injury Model

To explore further the regulatory mechanisms of miR-539-5p, an IBS intestinal mucosal epithelial cell injury model was established using LPS. NCM460 cells were induced with varying concentrations of LPS, revealing a marked rise in the apoptotic rate of these cells as the concentration of LPS escalated (Figure 2A). This was accompanied by a notable upregulation in apoptotic markers mRNA expression (BAX and CASP3) and a downregulation of the expression of anti-apoptotic protein mRNA (*BCL2*) (Figure 2B). Additionally, the proliferative capacity of the cells decreased (Figure 2C), while paracellular permeability increased significantly (Figure 2D). The levels of pro-inflammatory cytokines in NCM460 cells also exhibited a marked elevation (Figure 2E). Notably, with increasing LPS concentration, the expression of miR-539-5p significantly was down-regulated (Figure 2F).

### The Role of miR-539-5p LPS-Induced NCM460 Cell

To further clarify the impact of miR-539-5p in the damage of intestinal mucosal epithelial cells induced by LPS, the expression of miR-539-5p was successfully adjusted by transfection with mimics and inhibitors (Figure 3A). In the LPS-induced cellular model, it was found that miR-539-5p overexpression reduced the apoptotic capacity of NCM460 cells (Figures 3B-C), enhanced their proliferative ability (Figure 3D), inhibited paracellular permeability (Figure 3E), and alleviated the inflammatory response exhibited by NCM460 cells (Figure 3F). Conversely, knocking down miR-539-5p expression produced the opposite effects.

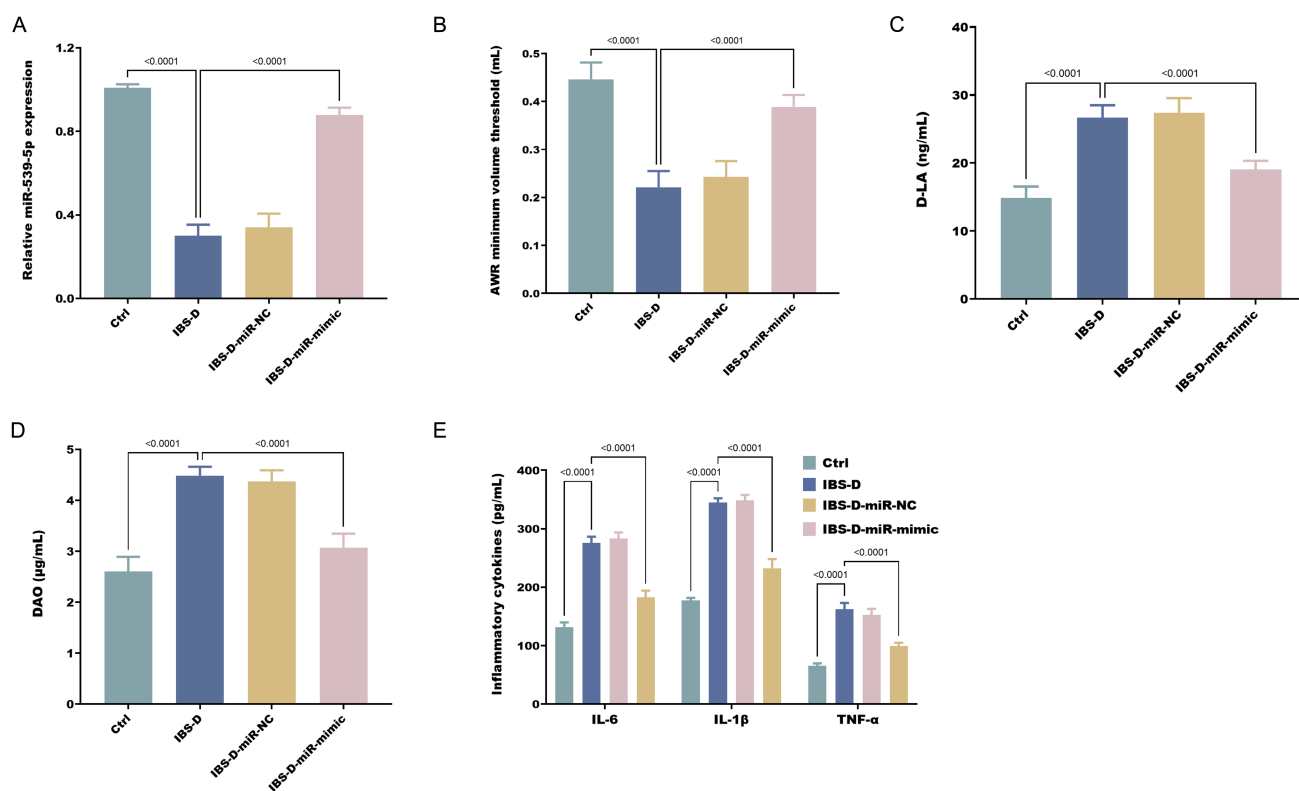


**Figure 1.** miR-539-5p is significantly downregulated in IBS-D rats (A), and its overexpression enhances AWR minimum volume threshold (B), reduces serum D-LA (C), DAO (D), and inflammatory cytokine levels (E) in IBS-D rats.

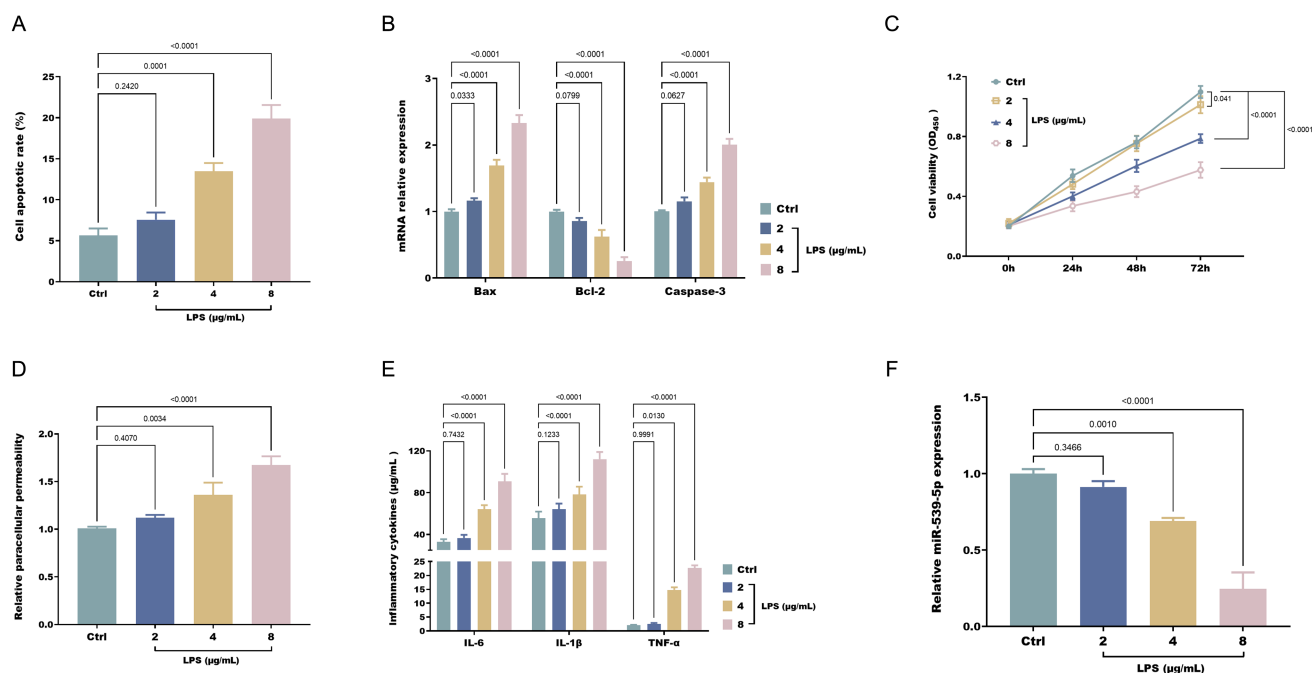


**Figure 2.** LPS induces apoptosis in NCM460 cells (A), upregulates apoptotic markers *BAX* and *CASP3* mRNA, downregulates anti-apoptotic markers *BCL2* mRNA (B), inhibits cell proliferation (C), increases paracellular permeability (D), promotes inflammation (E), and suppresses miR-539-5p expression (F).

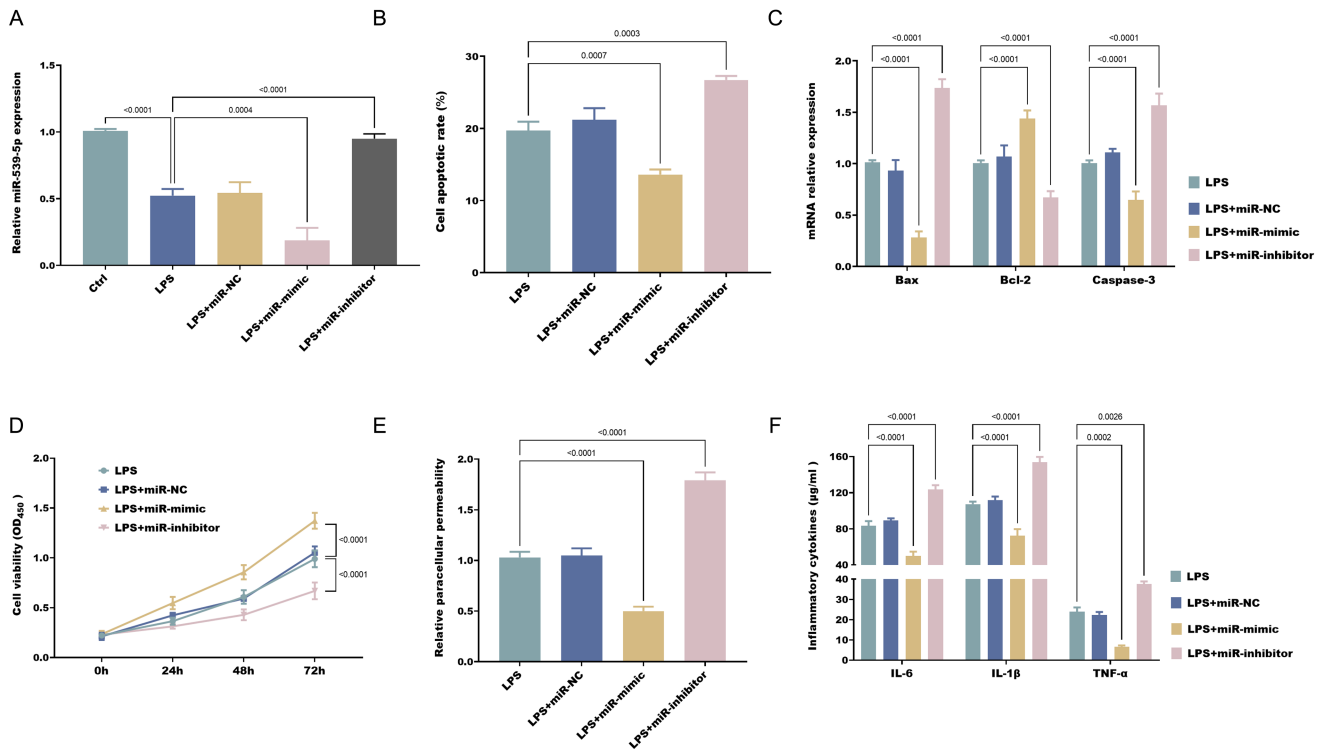


**Figure 3.** miR-539-5p expression is modulated by transfection with miR-539-5p mimics or inhibitors (A). miR-539-5p negatively regulates apoptosis (B-C) and positively regulates proliferation (D) in LPS-exposed NCM460 cells, while negatively regulating paracellular permeability (E) and pro-inflammatory cytokine secretion (F).

### Validation of miR-539-5p Targeting KDM6A

To elucidate the downstream targets of miR-539-5p, an intersection analysis was conducted using the Target Scan Human, miRDB, and miRwalk datasets, resulting in the identification of 56 common target genes (supplementary figure 1A). Functional annotation through GO (supplementary figure 1B) and KEGG (supplementary figure 1C) pathways revealed that these mRNAs were predominantly enriched in intestinal function, immune response, and neuroregulation. Protein-protein interaction analysis confirmed the direct interactions among these target genes ( $P < .05$ ), with KDM6A protein emerging as a pivotal hub within the network (supplementary figure 1D). Further investigation demonstrated that LPS stimulation induced the expression of *KDM6A* in NCM460 cells.

Additional research has shown that the expression of *Kdm6a* is markedly upregulated in IBS-D rats (Figure 4A). Furthermore, LPS stimulation can induce the expression of *KDM6A* in NCM460 cells (Figure 4B). Preliminary analysis revealed that miR-539-5p negatively regulates the relative luciferase activity of WT-*KDM6A* (Figure 4C). Moreover, in a cellular model induced by LPS,

the transfection with miR-539-5p mimics led to a notable decrease in *KDM6A* expression (Figure 4D).

### The Role of KDM6A LPS-Induced NCM460 Cell

In the LPS-induced cellular model, overexpression of *KDM6A* significantly reversed the positive effects elicited by miR-539-5p upregulation in NCM460 cells. Specifically, *KDM6A* upregulation promoted apoptotic capacity (Figure 5A-B), inhibited cell viability (Figure 5C), increased paracellular permeability (Figure 5D), and exacerbated inflammatory responses (Figure 5E) in NCM460 cells.

### DISCUSSION

Irritable bowel syndrome, a prevalent chronic functional gastrointestinal disorder, exhibits a complex and yet incompletely elucidated pathogenesis. In recent years, the role of miRNAs in regulating gene expression, cellular functions, and pathophysiological processes has garnered increasing attention.<sup>22,23</sup> This study aimed to initially investigate the role of miR-539-5p in the pathophysiology of IBS-D. An IBS-D mouse model was established as an experimental platform, with the AWR assessment

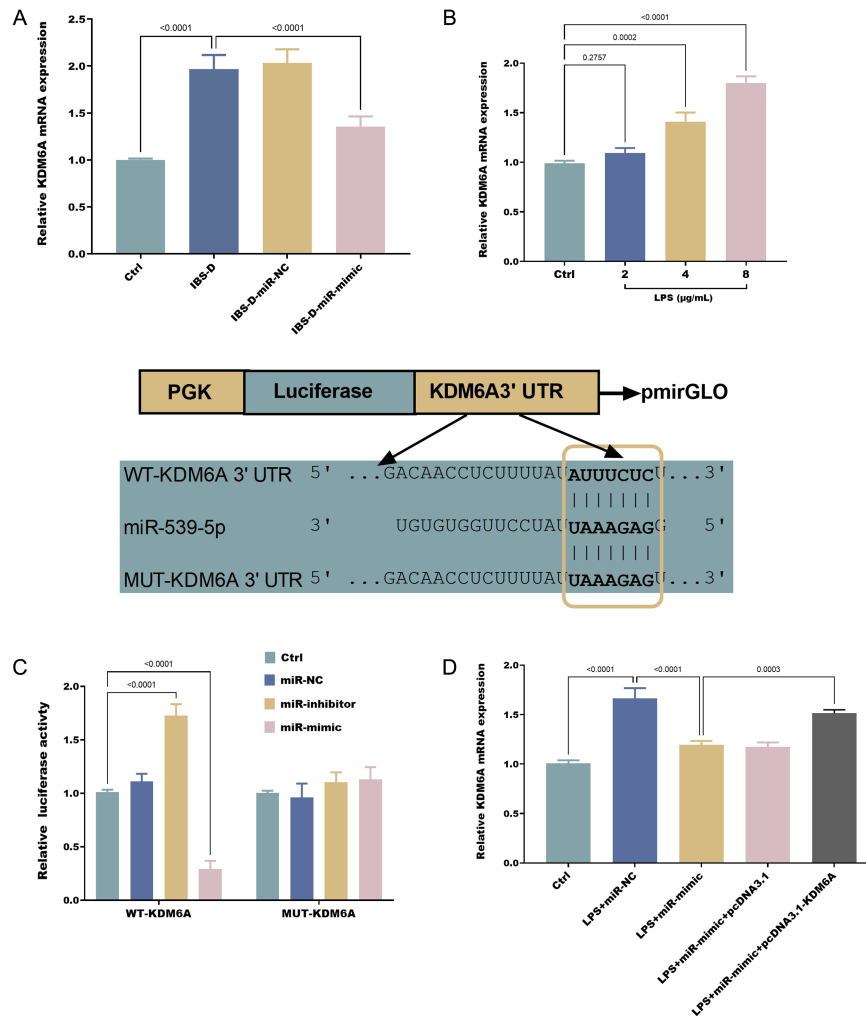


**Figure 4.** Kdm6a mRNA is significantly upregulated in IBS-D rats (A) and LPS-exposed NCM460 cells (B). Dual-luciferase reporter assay confirms the binding relationship between miR-539-5p and KDM6A in NCM460 cells (C). Overexpression of miR-539-5p inhibits KDM6A mRNA expression in LPS-exposed NCM460 cells (D).

system systematically introduced as a pivotal indicator of intestinal sensitivity.<sup>24</sup> Research indicates that D-LA is a metabolite generated by intestinal bacteria. In the event of intestinal mucosal injury, significant amounts of D-LA can permeate into the bloodstream.<sup>25</sup> Meanwhile, DAO represents an active enzyme that resides within intestinal mucosal cells. When these cells suffer damage, DAO is released into the circulatory system.<sup>26</sup> Elevated levels of both D-LA and DAO display a close correlation with the extent of intestinal mucosal damage as well as changes in permeability.<sup>27</sup> Furthermore, abnormal elevations in inflammatory cytokines such as IL-6, IL-1 $\beta$ , and TNF- $\alpha$  are also closely associated with significant impairment of intestinal barrier function.<sup>28</sup> Crucially, the study found miR-539-5p expression to be significantly downregulated

in model mice. Furthermore, miR-539-5p overexpression significantly improved AWR minimum volume threshold, reduced D-LA and DAO levels, and alleviated intestinal inflammatory responses. These findings suggest that miR-539-5p has a crucial regulatory role in the pathogenesis of IBS-D.

To preliminary investigate the specific regulatory mechanisms of miR-539-5p, an IBS cellular model was established by treating intestinal mucosal epithelial cells with exogenous LPS. Previous studies have confirmed that LPS treatment significantly inhibits intestinal mucosal epithelial cell viability, enhances paracellular permeability, and promotes cell apoptosis and inflammation.<sup>29</sup> Similarly, these phenomena were also observed in this



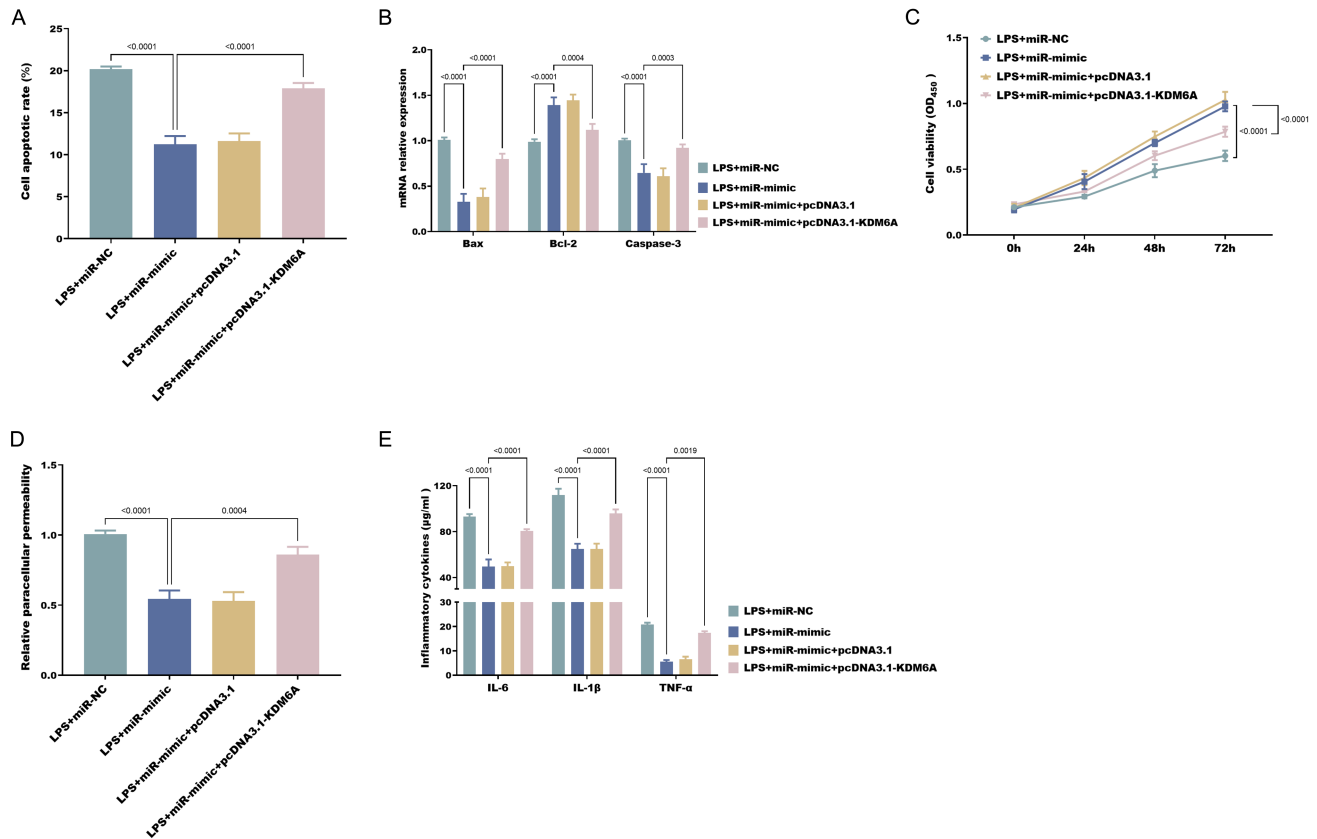


**Figure 5.** Overexpression of *KDM6A* significantly promotes apoptosis (A-B), inhibits proliferation (C), increases paracellular permeability (D), and promotes pro-inflammatory cytokine secretion (E) in LPS-exposed cells.

study. Notably, following LPS treatment, the expression of miR-539-5p was markedly downregulated. This discovery indicates that miR-539-5p could have a function in the process involving LPS-induced damage to intestinal mucosal epithelial cells. The results of this study demonstrate that the promotion of miR-539-5p expression can markedly alleviate the impact of LPS on the behavioral activities of intestinal mucosal epithelial cells, including restoring cell viability, reducing paracellular permeability, and decreasing cell apoptosis. Research has pointed out that the expression of miR-539-5p is markedly elevated in colorectal cancer tissues, and inhibiting its expression can restrain the proliferation and migration abilities of colorectal cancer cells and simultaneously induce apoptosis.<sup>30</sup> Similarly, miR-539-5p has been discovered to regulate the proliferation and migration in vascular smooth muscle cells stimulated by ox-LDL by targeting SPP1.<sup>12,31</sup> These studies provide further evidence to support the assertion that miR-539-5p plays a pivotal role in the behavioral activities of intestinal mucosal epithelial cells. Moreover, this study also discovered that miR-539-5p

can negatively regulate the inflammatory response of LPS-induced intestinal mucosal epithelial cells. In the acute lung injury model, overexpression of miR-539-5p can mitigate the inflammatory response of LPS-induced pulmonary microvascular endothelial cells.<sup>32</sup> In the sepsis cell model, miR-539-5p has also been found to regulate the levels of TNF- $\alpha$  and IL-1 $\beta$  in cardiomyocytes.<sup>33</sup> The collective evidence indicates that miR-539-5p may act as a responsive molecule under LPS stimulation and participate in the regulation of the cellular inflammatory response process.

It was determined that the *KDM6A* serves as a target of miR-539-5p and was notably upregulated in IBS-D mice. *KDM6A*, a cell adhesion molecule, is vital for maintaining intercellular connections and barrier functions.<sup>34,35</sup> The findings of this research indicate that the promotion of *KDM6A* expression may serve to reverse the protective effect of miR-539-5p upregulation on intestinal mucosal epithelial cells. Similarly, in the spinal cord injury model, the high expression of *KDM6A* coexisted with the

damaged response of nerve cells, and miR-145 exhibited a neuroprotective effect by regulating the expression of *KDM6A*.<sup>36</sup> Additionally, study on type 1 diabetic nephropathy have shown a correlation between elevated *KDM6A* levels and worsened renal tubular dysfunction and tissue damage, with miR-199b-3p downregulation accelerating the epithelial-to-mesenchymal transition process by influencing *KDM6A* and E-cadherin expression.<sup>37</sup> The above shows that *KDM6A*, as a key node in the microRNA regulatory network, exerts a significant influence on the regulation of cell fate and tissue repair.

While this study offers initial insights into the role of miR-539-5p and *KDM6A* in IBS, it has several limitations. Firstly, immunohistochemical analysis of tight junction markers to assess intestinal permeability was not conducted. Such analysis could have provided a more detailed and direct visualization of changes in intestinal barrier function, strengthening the evidence for a connection between miR-539-5p and intestinal mucosal integrity. Additionally, further analyses of the signaling pathways involved have not been conducted. Lastly, feces samples could have provided valuable information regarding changes in the gut microbiota and intestinal permeability markers, further enriching our understanding of the role of miR-539-5p in IBS. The feces of all IBS-D rats included in this study exhibited typical diarrhea manifestations, such as pasty, loose, or watery consistency. However, difficulties were encountered when attempting to collect samples from these diarrhea rat models. The inherent complexity of feces sample collection, coupled with its susceptibility to contamination, resulted in inconsistent and unsatisfactory outcomes. Future research should address these limitations to fully elucidate the role of miR-539-5p in IBS.

In summary, miR-539-5p likely impacts the function of intestinal mucosal epithelial cells by regulating downstream target genes such as *KDM6A*, thereby participating in the onset and progression of IBS. Future research can delve deeper into the interaction mechanisms between miR-539-5p and *KDM6A*, as well as their potential therapeutic applications in IBS.

**Data Availability Statement:** The data that support the findings of this study are available on request from the corresponding author.

**Ethics Committee Approval:** This study was approved by the Ethics Committee of Xuzhou Medical University (approval number: 202503T030; date: February 15, 2025).

**Informed Consent:** N/A.

**Peer-review:** Externally peer-reviewed.

**Author Contributions:** Concept – L.L.; Design – Y.L.; Supervision – L.L.; Resources – Y.H.; Materials – S.Z.; Data Collection and/or Processing – Y.L., Z.W., S.Z., Y.H.; Analysis and/or Interpretation – Y.L., Z.W., L.L.; Literature Search – Y.H., X.T.F.; Writing – Y.L.; Critical Review – L.L.

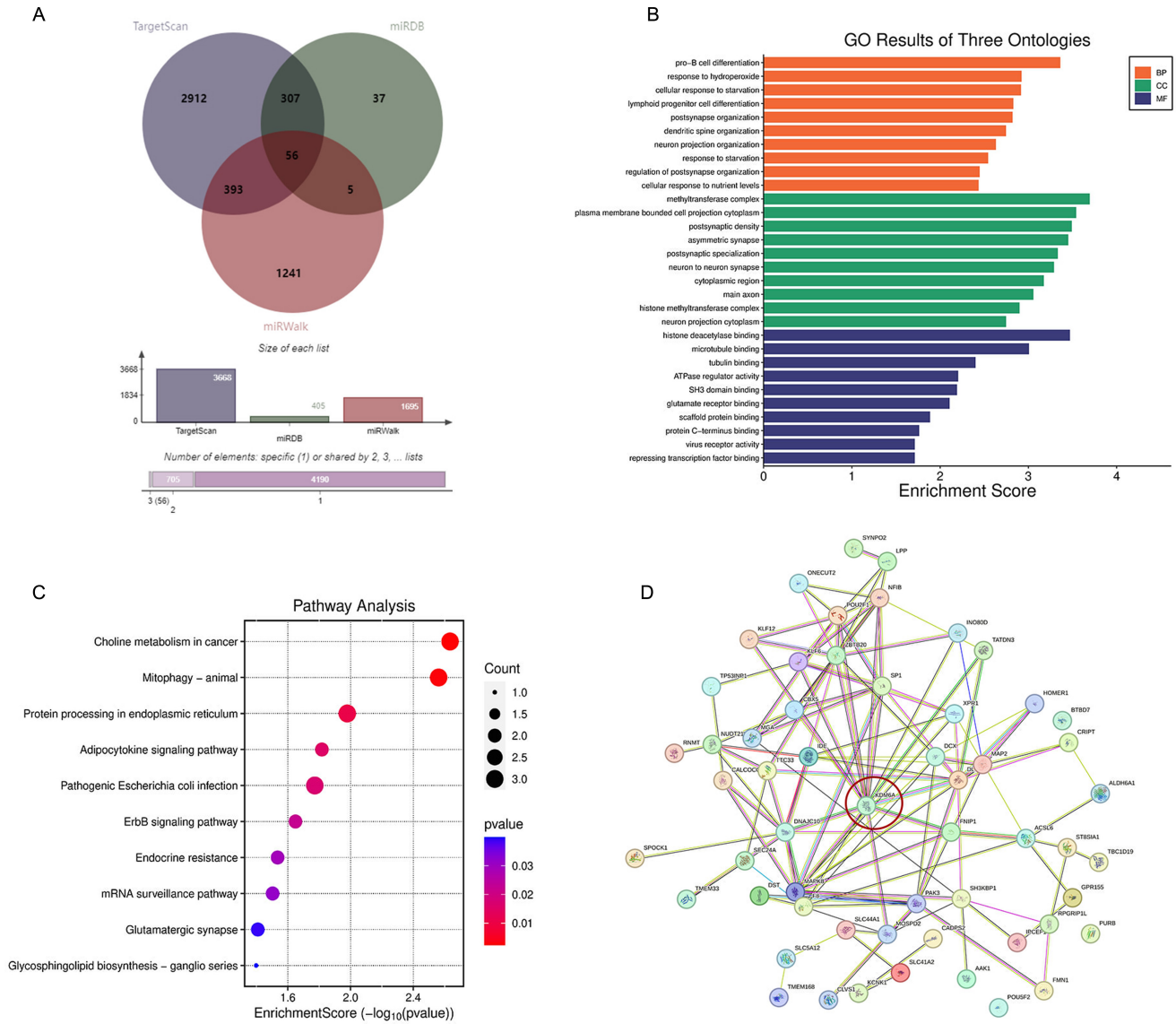
**Declaration of Interests:** The authors have no conflicts of interest to declare.

**Funding:** This study received no funding.

## REFERENCES

1. Saha L. Irritable bowel syndrome: pathogenesis, diagnosis, treatment, and evidence-based medicine. *World J Gastroenterol*. 2014;20(22):6759-6773. [\[CrossRef\]](#)
2. Holtmann GJ, Ford AC, Talley NJ. Pathophysiology of irritable bowel syndrome. *Lancet Gastroenterol Hepatol*. 2016;1(2):133-146. [\[CrossRef\]](#)
3. Akyüz F, Çelebi A, Doğan İ, et al. Functional bowel disorder management in routine practice with tips for hot topics: expert opinion review. *Turk J Gastroenterol*. 2024;35(6):423-439. [\[CrossRef\]](#)
4. Camilleri M, Boeckstaens G. Irritable bowel syndrome: treatment based on pathophysiology and biomarkers. *Gut*. 2023;72(3):590-599. [\[CrossRef\]](#)
5. Defrees DN, Bailey J. Irritable bowel syndrome: epidemiology, pathophysiology, diagnosis, and treatment. *Prim Care*. 2017;44(4):655-671. [\[CrossRef\]](#)
6. Fourie NH, Peace RM, Abey SK, et al. Elevated circulating miR-150 and miR-342-3p in patients with irritable bowel syndrome. *Exp Mol Pathol*. 2014;96(3):422-425. [\[CrossRef\]](#)
7. Cheng X, Zhang X, Su J, et al. miR-19b downregulates intestinal SOCS3 to reduce intestinal inflammation in Crohn's disease. *Sci Rep*. 2015;5:10397. [\[CrossRef\]](#)
8. Guo JG, Rao YF, Jiang J, Li X, Zhu SM. MicroRNA-155-5p inhibition alleviates irritable bowel syndrome by increasing claudin-1 and ZO-1 expression. *Ann Transl Med*. 2023;11(2):34. [\[CrossRef\]](#)
9. Zhou Q, Yang L, Larson S, et al. Decreased miR-199 augments visceral pain in patients with IBS through translational upregulation of TRPV1. *Gut*. 2016;65(5):797-805. [\[CrossRef\]](#)
10. Feng Y, Wang J, Yuan Y, Zhang X, Shen M, Yuan F. miR-539-5p inhibits experimental choroidal neovascularization by targeting CXCR7. *FASEB J*. 2018;32(3):1626-1639. [\[CrossRef\]](#)
11. Dai Q, Shi R, Zhang G, et al. miR-539-5p targets BMP2 to regulate Treg activation in B-cell acute lymphoblastic leukemia through TGF-β/Smads/MAPK. *Exp Biol Med (Maywood)*. NJ. 2024;249:10111. [\[CrossRef\]](#)
12. Liu SL, Chen MH, Wang XB, et al. LncRNA PCGEM1 contributes to malignant behaviors of glioma by regulating miR-539-5p/CDK6 axis. *Aging*. 2021;13(4):5475-5484. [\[CrossRef\]](#)
13. Gong T, Li Y, Feng L, et al. CASC21, a FOXP1 induced long non-coding RNA, promotes colorectal cancer growth by regulating CDK6. *Aging*. 2020;12(12):12086-12106. [\[CrossRef\]](#)
14. Zhang Y, Wu Z. LINC02605 involved in paediatric *Mycoplasma pneumoniae* pneumonia complicated with diarrhoea via miR-539-5p/CXCL1 axis. *Eur J Clin Invest*. 2024;54(9):e14234. [\[CrossRef\]](#)

15. Wang D, Xue H, Tan J, et al. Bone marrow mesenchymal stem cells-derived exosomes containing miR-539-5p inhibit pyroptosis through NLRP3/caspase-1 signalling to alleviate inflammatory bowel disease. *Inflam Res Off J Eur Histamine Res Soc.* 2022;71(7-8):833-846. [\[CrossRef\]](#)
16. Wang Y, Ke W, Gan J, et al. MicroRNA-29b-3p promotes intestinal permeability in IBS-D via targeting TRAF3 to regulate the NF- $\kappa$ B-MLCK signaling pathway. *PLoS One.* 2023;18(7):e0287597. [\[CrossRef\]](#)
17. Zhu H, Xiao X, Shi Y, et al. Inhibition of miRNA-29a regulates intestinal barrier function in diarrhea-predominant irritable bowel syndrome by upregulating ZO-1 and CLDN1. *Exp Ther Med.* 2020;20(6):155. [\[CrossRef\]](#)
18. Zhang Y, Wu X, Wu J, et al. Decreased expression of microRNA-510 in intestinal tissue contributes to post-infectious irritable bowel syndrome via targeting PRDX1. *Am J Transl Res.* 2019;11(12):7385-7397
19. De Gregorio A, Serafino A, Krasnowska EK, et al. Protective effect of *Limosilactobacillus fermentum* ME-3 against the increase in paracellular permeability induced by chemotherapy or inflammatory conditions in Caco-2 cell models. *Int J Mol Sci.* 2023;24(7):6225. [\[CrossRef\]](#)
20. Kida R, Tsugane M, Suzuki H. Horizontal and vertical micro-chamber platforms for evaluation of the paracellular permeability of an epithelial cell monolayer. *Lab Chip.* 2024;24(3):572-583. [\[CrossRef\]](#)
21. Armstrong SM, Khajoe V, Wang C, et al. Co-regulation of trans-cellular and paracellular leak across microvascular endothelium by dynamin and Rac. *Am J Pathol.* 2012;180(3):1308-1323. [\[CrossRef\]](#)
22. Ji LJ, Li F, Zhao P, et al. Silencing interleukin 1 $\alpha$  underlies a novel inhibitory role of miR-181c-5p in alleviating low-grade inflammation of rats with irritable bowel syndrome. *J Cell Biochem.* 2019;120(9):15268-15279. [\[CrossRef\]](#)
23. Guo J, Lu G, Chen L, et al. Regulation of serum microRNA expression by acupuncture in patients with diarrhea-predominant irritable bowel syndrome. *Acupunct Med.* 2022;40(1):34-42. [\[CrossRef\]](#)
24. Lin M, Hu G, Wang Z, Yu B, Tan W. Activation of the high-affinity choline Transporter 1 in the spinal cord relieves stress-induced hyperalgesia. *Dig Dis Sci.* 2023;68(6):2414-2426. [\[CrossRef\]](#)
25. Cai Y, Gong D, Xiang T, Zhang X, Pan J. Markers of intestinal barrier damage in patients with chronic insomnia disorder. *Front Psychiatry.* 2024;15:1373462. [\[CrossRef\]](#)
26. Xu Y, Yao R, Zhao W, et al. Spirocyclopiperazinium salt compound DXL-A-24 improves visceral sensation and gut microbiota in a rat model of irritable bowel syndrome. *Heliyon.* 2023;9(6):e16544. [\[CrossRef\]](#)
27. Liu M, Wang Y, Xu X, et al. p-hydroxy benzaldehyde attenuates intestinal epithelial barrier dysfunction caused by colitis via activating the HNF-1 $\beta$ /SLC26A3 pathway. *Front Pharmacol.* 2024;15:1448863. [\[CrossRef\]](#)
28. Zhao K, Yu L, Wang X, He Y, Lu B. *Clostridium butyricum* regulates visceral hypersensitivity of irritable bowel syndrome by inhibiting colonic mucous low grade inflammation through its action on NLRP6. *Acta Biochim Biophys Sin (Shanghai).* 2018;50(2):216-223. [\[CrossRef\]](#)
29. Wu J, He C, Bu J, et al. Betaine attenuates LPS-induced down-regulation of occludin and Claudin-1 and restores intestinal barrier function. *BMC Vet Res.* 2020;16(1):75. [\[CrossRef\]](#)
30. Ding C, Zhang K, Chen Y, Hu H. LncRNA TP73-AS1 enhances the malignant properties of colorectal cancer by increasing SPP-1 expression through miRNA-539-5p sponging. *Pathol Res Pract.* 2023;243:154365. [\[CrossRef\]](#)
31. Zhang Y, Tang Y, Yan J. LncRNA-XIST promotes proliferation and migration in ox-LDL stimulated vascular smooth muscle cells through miR-539-5p/SPP1 axis. *Oxid Med Cell Longev.* 2022;2022:9911982. [\[CrossRef\]](#)
32. Meng L, Cao H, Wan C, Jiang L. MiR-539-5p alleviates sepsis-induced acute lung injury by targeting ROCK1. *Folia Histochem Cytobiol.* 2019;57(4):168-178. [\[CrossRef\]](#)
33. Hu X, Miao H. MiR-539-5p inhibits the inflammatory injury in septic H9c2 cells by regulating IRAK3. *Mol Biol Rep.* 2022;49(1):121-130. [\[CrossRef\]](#)
34. Kong N, Zhang R, Wu G, et al. Intravesical delivery of KDM6A-mRNA via mucoadhesive nanoparticles inhibits the metastasis of bladder cancer. *Proc Natl Acad Sci U S A.* 2022;119(7):e2112696119. [\[CrossRef\]](#)
35. Li D, Zhang S, Yan Q, Li Y. Lysine-specific demethylase 6A upregulates Cadherin-1 and accelerates gastric cancer growth. *Curr Pharm Biotechnol.* 2023;24(14):1827-1835. [\[CrossRef\]](#)
36. Gao C, Yin F, Li R, et al. MicroRNA-145-Mediated KDM6A down-regulation enhances neural repair after spinal cord injury via the NOTCH2/Abcb1a axis. *Oxid Med Cell Longev.* 2021;2021:2580619. [\[CrossRef\]](#)
37. Bai S, Xiong X, Tang B, et al. hsa-miR-199b-3p Prevents the Epithelial-Mesenchymal Transition and Dysfunction of the Renal Tubule by Regulating E-cadherin through Targeting KDM6A in Diabetic Nephropathy. *Oxid Med Cell Longev.* 2021;2021:8814163. [\[CrossRef\]](#)



**Supplementary Figure 1.** A Total of 56 miR-539-5p target genes were obtained by intersecting 3 databases. GO (B) and KEGG (C) perform functional enrichment analysis on target genes. PPI analysis of target genes (D).

**Supplementary Table 1.** Reverse reaction system (20μL system)

Name	Dosage
Total RNA (DNA removal)	2 μg
Prime Script RT Enzyme Mix I	1 μL
Random 6 mers (100μM)	1 μL
Oligo dT Primer (50μM)	1 μL
5×Prime Script Buffer 2	4 μL
Rnase Free dH <sub>2</sub> O	11 μL

**Supplementary Table 2.** RT-qPCR reaction system (20μl system)

Name	Dosage
2×SYBR Premix Ex Taq II (Tli Rnase Plus)	10 μL
Forward primer (10uM)	0.8 μL
Reverse primer (10uM)	0.8 μL
cDNA (5uM)	2 μL
Rnase Free dH <sub>2</sub> O	6.4 μL

**Supplementary Table 3.** The reaction condition of RT-qPCR

Steps	Temperature	Time	Cycle
Pre-denaturation	95°C	30s	1
Denaturation	95°C	5s	40
Annealing	60°C	30	
Extension	72°C	30	1

**Supplementary Table 4.** Primer sequences

Primer Name		Primer sequence
KDM6A	forward	5'-TTTGGTCTACTTCCATTACAATGCA-3'
	reverse	5'-AAGCCCAAGTCGTAAATGAATTTTC-3'
Bax	forward	5' CGGCGAATTGGAGATGAACTGG3'
	reverse	5'CTGCAGAGGATGATTGCTGA3'
Caspase-3	forward	5'-GCTATTGTGAGGCGGTTGT-3'
	reverse	5'-TGTTTCCCTGAGGTTTGC-3'
Bcl-2	forward	5'-TACCGTCGTGACTTCGCAGAGAT-3'
	reverse	5'-AGGAGAAATCAAACAGAGGTCGC-3'
GAPDH	forward	5'-GGGCATCTTGGGCTACAC-3'
	reverse	5'-GGTCCAGGGTTTCTTACTCC-3'
miR-539-5p	forward	5'-CCAAAGGAGCATCAGA GCAGA-3'
	reverse	5'-AAGGGCTCGACAGAATTGGG-3'
U6	forward	5'-CTCGCTTCGGCAGCACA-3
	reverse	5'-AACGCTTCACGAATTTGCGT-3'

KDM6A: Lysine Demethylase 6A; Bcl-2: B-cell lymphoma-2; Bax: BCL-2-associated X protein;